Conformation of Parathyroid Hormone: Time-Resolved Fluorescence Studies†

K. J. Willis‡,§ and A. G. Szabo*,§

Allelix Biopharmaceuticals Inc., 6850 Goreway Drive, Mississauga, Ontario, Canada L4V 1P1, and The Centre for Protein Structure and Design, National Research Council of Canada, Ottawa, Ontario, Canada K1A 0R6

Received April 9, 1992; Revised Manuscript Received June 26, 1992

ABSTRACT: Conformational and environmental changes in the functionally significant amino-terminal region of human parathyroid hormone (hPTH), induced by solvent or by complexation with acidic lipid, have been investigated. Structural perturbations were monitored by their effect on the fluorescence decay kinetics of the single tryptophyl residue at position 23. Data for the intact hormone were compared with those for its 1–34 and 13–34 analogues. Deletion of the 35–84 sequence had no significant effect on the structure of hPTH in the region of Trp-23, nor was there any evidence for interaction of this region with the 1–12 sequence. On the basis of a comparison of the results of this study with structural information available from other spectroscopic techniques, we propose that the local structure in the region of Trp-23 of aqueous solutions of hPTH and hPTH 1–34 has helical character. This local structure was not stable in aqueous hPTH 13–34, but was present in hPTH and its analogues, both on complexation with acidic lipid and in helix-promoting solvents. The tryptophyl fluorescence of the lipid-bound peptides was characteristic of an aqueous environment. Triple-exponential fluorescence decay kinetics were observed for the tryptophyl residue of hPTH and its deletion analogues. This can be explained in terms of ground-state heterogeneity due to the presence of three C_α–C_β rotamers of the tryptophanyl indole side chain. Assuming this model, we show that the calculated fractional concentrations of the decay time components correlate with the likely rotamer populations and with their expected dependence on the main-chain conformation. This analysis demonstrates that information on secondary structure is available from time-resolved fluorescence data.

Parathyroid hormone (PTH)[1] maintains calcium and phosphate homeostasis as a result of its key role in regulating the intestinal absorption, renal excretion, and bone deposition/resorption of both minerals. The native hormone is a linear peptide of 84 amino acids, although it is apparent that the 1–34 sequence contains the biological information for nearly all of the major physiological properties of PTH. Extensive investigation of the structural requirements for receptor binding and biological activity has identified several functionally important domains within the 1–34 sequence. The first few residues of the N-terminal region are associated with the stimulation of adenylate cyclase activity, which was thought to be the predominant second-messenger mechanism for PTH. The 10–15 and, perhaps more significantly, the 24–34 regions appear to be important for receptor binding [for reviews, see Potts et al. (1982), Habener et al. (1984), and Jüppner (1989)].

It has recently been established that in addition to its ability to activate adenylate cyclase, PTH also triggers a mechanism leading to increase in membrane-associated protein kinase C (PKC) activity (Chakravarthy et al., 1990; Nemani et al., 1991; Jouishomme et al., 1991). This may in turn mediate many of the important PTH functions. The PKC activation domain is suggested to be located in the region of residues 28–34 (Jouishomme et al., 1991). However, many of the biological actions of PTH, including binding to the same receptor, are mimicked by a tumor-secreted hormone, parathyroid hormone related protein (PTHrP) (Jüppner, 1989; Caulfield et al., 1990; Evely et al., 1991; Martin et al., 1991, and references cited therein), and yet the primary structure of PTHrP is homologous to PTH only in the region of the N-terminus, where 8 of the first 13 residues are identical (Suva et al., 1987).

The structural basis for the various PTH domains and their emulation by PTHrP is not fully understood, due in part to the lack of detailed information on the conformation of these hormones. Theoretical studies (Zull & Lev, 1980; Cohen et al., 1991) predict extensive secondary structure for the PTH 1–34 fragment, comprised largely of 2 ca. 10-residue helicies. Evaluation of the α-helical content of PTH 1–34 by circular dichroism (CD) suggests 7–11 residues are in a helical conformation in aqueous solution (Hong et al., 1986; Zull et al., 1990; Cohen et al., 1991). In a solution of 40% (v/v) trifluoroethanol (TFE), the helical content increases to 24–26 residues (Cohen et al., 1991). Cohen et al. (1991) also compared the CD spectra of PTH 1–34 with PTHrP 1–34 and concluded that they have very similar secondary structural features. According to NMR, PTH 1–34 in 11% TFE (aqueous) contains two α-helicies (residues 3–9 and 17–28) linked by a nonstructured region (Klaus et al., 1991). In aqueous solution, NMR investigations have suggested PTH 1–34 is in an extended flexible form with the exception of a local "non-random" structure in the region of Trp-23 (Bundi et al., 1976, 1978; Lee & Russel, 1989). Other NMR data apparently support a more ordered structure for PTH (Smith et al., 1987; Coddington & Barling, 1989) and PTHrP (Barden & Kemp, 1989) in aqueous solution. It is clear, therefore, that there is little consensus on the structural properties of these interesting and important hormones.

† Issued as NRCC Publication No. 34272. This work was partially funded by an NRC–Allelix Biopharmaceuticals Inc. biotechnology contribution program comprehensive agreement.

* To whom correspondence should be addressed.

‡ Allelix Biopharmaceuticals Inc.

§ National Research Council of Canada.

[1] Abbreviations: PTH, parathyroid hormone; h, human; r, rat; PKC, protein kinase C; PTHrP, parathyroid hormone related protein; CD, circular dichroism; TFE, trifluoroethanol; NMR, nuclear magnetic resonance; POPS, 1-palmitoyl-2-oleoylphosphatidylserine; HPLC, high-performance liquid chromatography; ESI, electrospray ionization; DAS, decay-associated spectra; M_w, molecular weight; GuHCl, guanidine hydrochloride; NATA, *N*-acetyltryptophanamide.

0006-2960/92/0431-8924$03.00/0 Published 1992 by the American Chemical Society

Human (h) PTH contains a single tryptophan residue at position 23 and no tyrosine residues. In this paper, we have used Trp-23 as a fluorescent probe to investigate the conformational and environmental modifications induced in hPTH by sequence deletion, by changes in solvent composition, and by complexation with acidic lipid vesicles. The changes in the Trp-23 fluorescence parameters allow us to elucidate the structural details of a functionally significant region of PTH.

EXPERIMENTAL PROCEDURES

Materials. Recombinant hPTH was a gift of Dr. A. Kronis of Allelix Biopharmaceuticals Inc. (Mississauga, Ontario, Canada). hPTH 1–34 (lot ZG724), hPTH 13–34 (lot ZE591), and rat (r) PTH 1–34 (lot ZH521) were purchased from Bachem (Torrance, CA). 1-Palmitoyl-2-oleoylphosphatidylserine (POPS) was purchased from Avanti Polar Lipids (Birmingham, AL). All other chemicals were of analytical grade and were used without further purification.

Mass Spectroscopy. All peptides were "pure" by the criterion of analytical reverse-phase HPLC. The following samples were also subjected to mass spectrometry to further confirm their identity and purity: hPTH, hPTH 1–34, and hPTH 13–34. Mass spectrometry was performed on an AT1 Model 3 quadrupole instrument (Sciex, Ontario, Canada) employing nebulization-assisted electrospray ionization (ESI) from a 0.5 mg/mL solution in 10% HOAc.

Sample Preparation. Peptide samples were prepared by dissolving the peptide in 1 mM phosphate adjusted to pH 3.0 with HCl. The pH was then increased by the addition of small amounts of NaOH. Unilamellar POPS vesicles in 1 mM phosphate, pH 7.5, of ca. 100-nm diameter were prepared at ambient temperature as described by Cavatorta et al. (1991). The vesicle size distribution was analyzed using a Nicomop 370 particle sizing system.

Spectroscopic Measurements. CD spectroscopy was performed as described by Zull et al. (1990) except that PTH peptides were first solubilized in low-pH solutions. Time-resolved fluorescence measurements were conducted using the technique of time-correlated single proton counting with laser/microchannel plate based instrumentation. The instrumentation and procedures for time-resolved and steady-state meaurements have been given elsewhere (Szabo et al., 1989). Data were typically collected at 10 ps/channel in 2048 channels. The instrument response function was determined from the Raman scattering of the excitation (Willis et al., 1990), by water (at 328 nm for the 295-nm excitation), and had a fwhm of 60 ps. Each decay curve typically contained (1–2) × 10^6 total counts. All measurements were performed at 20 °C with a spectral resolution of 4 nm, and corrections were made for the signal from the appropriate "buffer only" blank. Procedures for the simultaneous or "global" (Knutson et al., 1983) analysis of multiple time-resolved data sets and criteria for assessing the quality of the fit have been described earlier (Willis & Szabo, 1989).

The function describing the fluorescence intensity decay following excitation was modeled as a sum of exponentials:

$$I(\lambda,t) = \sum_i \alpha_i(\lambda) \exp(-t/\tau_i) \quad (1)$$

where τ_i is the emission wavelength independent decay time of the ith decay component and $\alpha_i(\lambda)$ is its preexponential factor at emission wavelength λ. Initially it is assumed that the complex decay kinetics are the result of ground-state conformational heterogeneity. The emission spectra associated with each individual decay time component and hence each ground-state species (DAS, decay-associated spectra; Knutson et al., 1982) are given by

$$I_i(\lambda) = I_{ss}(\lambda)[\alpha_i(\lambda)\tau_i/\sum_i \alpha_i(\lambda)\tau_i] \quad (2)$$

where $I_i(\lambda)$ is the DAS of the ith component, $I_{ss}(\lambda)$ is the total steady-state spectrum, and its multiplier is the fractional fluorescence, f_i of the ith component at wavelength λ.

The DAS can be used to derive the relative concentrations of the ground-state species as

$$A_i = \int I_i(\lambda)\, d\lambda \quad (3)$$

where A_i is the area under the DAS of the ith component and furthermore

$$A_i \propto \epsilon_i(\lambda)\phi_i C_i \quad (4)$$

where $\epsilon_i(\lambda)$ is the extinction coefficient at the excitation wavelength, ϕ_i is the quantum yield, and C_i is the concentration of the ith component. It is expected that the absorption properties of the ground-state species will be similar since they presumably represent different conformers of the single fluorophore (Donzel et al., 1974). Therefore, equal extinction coefficients and radiative rate constants (Strickler & Berg, 1962) are assumed. Since $\phi_i = \tau_i/\tau_r$ where τ_r is the reciprocal of the radiative rate constant, then eq 4 reduces to $A_i \propto \tau_i C_i$. The fractional concentration of each ground-state species, c_i, is therefore

$$c_i = (A_i/\tau_i)/(\sum_i A_i/\tau_i) \quad (5)$$

To ensure the c_i's were determined with similar precision, data were collected at the same series of emission wavelengths in each experiment. We found that no significant error in the determination of the c_i's was introduced by sampling only the 310–420-nm region of the total emission spectrum.

RESULTS

Mass Spectrometry. The ESI mass spectra of hPTH 1–34, molecular weight (M_w) 4118, and hPTH 13–34, M_w 2808, were composed predominantly of peaks corresponding to the +4 to +7 and +3 to +6 protonated molecular ions, respectively. Both spectra showed weak contributions from peaks on the low m/z side, indicating the presence of molecules with M_w 3932 (for hPTH 1–34) or M_w 2679 (for hPTH 13–34). These M_w's are those expected for hPTH 3–34 and hPTH 14–34. The mass spectrum of hPTH confirmed its identity and purity (A. Kronis, personal communication).

Circular Dichroism. Circular dichroism spectra were recorded to monitor anticipated secondary structural changes induced by the perturbants utilized in the fluorescence studies. In our initial CD experiments, the lyophilized PTH peptides were dissolved in 1 mM phosphate buffer, pH 7. The resulting spectra, while similar in shape to those reported earlier (Zull et al., 1990), did not have reproducible ellipticities. Consistent results were obtained if the peptides were first dissolved at pH 3 and then titrated to the required pH. The CD spectra of hPTH 1–34 and hPTH 13–34 at acidic and neutral pH are shown in Figure 1. Spectra were found to be independent of concentration (2–130 μM) and ionic strength (1–200 mM, NaF). In a more detailed analysis, the mean residue ellipticity of hPTH 1–34 at both 195 and 222 nm varied with pH ($3.5 \leq pH \leq 8.5$) according to the Henderson–Hasselbalch equation with an apparent pK_a of 5.4 ± 0.1. The rPTH 1–34 showed very similar behavior.

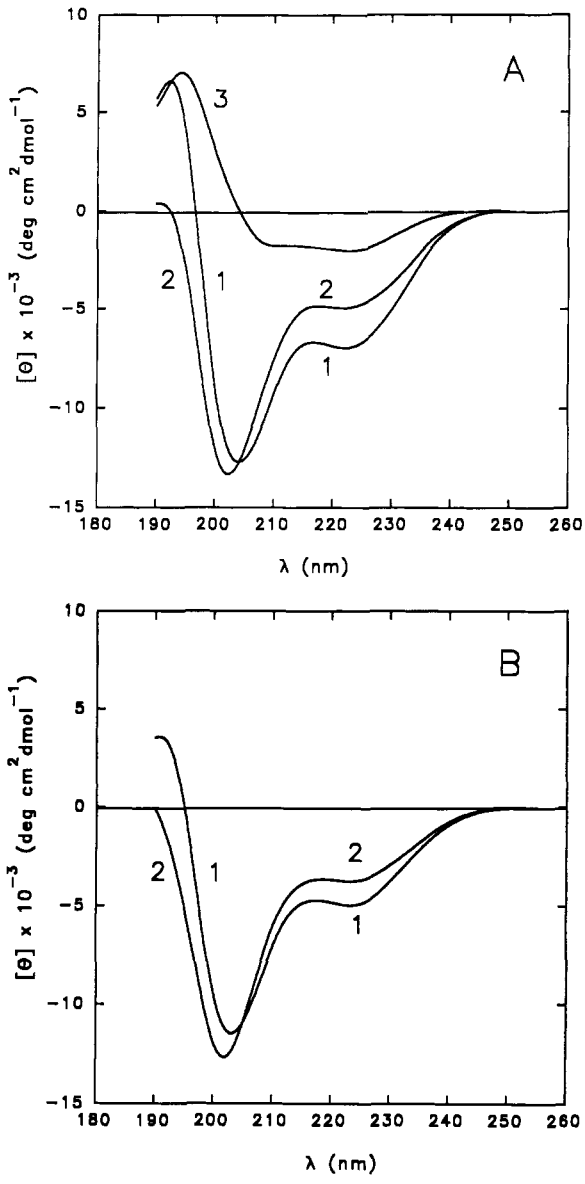

FIGURE 1: Circular dichroism spectra of hPTH deletion analogues at neutral and acidic pH. Peptide concentrations were typically 10 μM in 1 mM phosphate. The path length was 0.5 cm. (A) hPTH 1–34: (1) pH 7; (2) pH 3; (3) difference spectrum resulting from subtraction of the pH 3 spectrum from the pH 7 spectrum. (B) hPTH 13–34: (1) pH 7.1; (2) pH 3.

Addition of TFE (Cohen et al., 1991; Neugebauer et al., 1992) or complexation with acidic lipid vesicles (Neugebauer et al., 1992) is known to result in dramatic changes in the CD spectra of PTH peptides, consistent with an increase in the apparent α-helical content. Our CD data for PTH peptides in the presence of 35% TFE (1 mM phosphate, pH 7.5) or POPS vesicles (lipid:peptide ratio 50:1 in 1 mM phosphate, pH 7.5) were in accord with the published reports (data not shown). These data were collected only to confirm the structural changes had occurred, and detailed analyses of the CD spectra were not attempted. We note that Gaussian particle size analysis of the vesicles indicated mean diameters in the range 110–130 nm with standard deviations of 50 nm and that peptide binding had no significant effect on this distribution. As expected, the CD spectra of the PTH peptides in 6 M GuHCl were featureless, indicating the absence of organized secondary structure.

Time-Resolved Fluorescence. For all of the peptides studied, a triple-exponential law was required to satisfactorily fit the tryptophyl fluorescence decay data. Analysis of individual decay curves obtained at a series of wavelengths between 310 and 420 nm indicated that the decay times were independent of emission wavelength. Global analysis assuming three, wavelength-independent, decay times gave an excellent fit to the multiple emission wavelength data in all cases.[2] The results are presented in Table I. The fluorescence decay kinetics of hPTH and its deletion analogues have not been previously reported. They appear to be typical of an exposed tryptophyl residue in a flexible polypeptide (Eftink, 1991).

TFE promotes α-helix formation in PTH and its fragments (Cohen et al., 1991; Neugebauer et al., 1991). The increase in secondary structure reaches a plateau at approximately 35% TFE. In order to dissociate the consequences of solvent-induced conformational changes in the peptide structure on the fluorescence properties of the tryptophyl residue, from the general solvent effect on the fluorophore, the model compound *N*-acetyltryptophanamide (NATA) was studied in the same TFE solutions. NATA in 1 mM phosphate buffer, pH 7.5, exhibited single-exponential decay kinetics with a lifetime of 3.03 ns (380-nm emission). In the same buffer containing 35% TFE, the NATA fluorescence decay data gave an acceptable fit to a lifetime of 2.27 ns, a 1.33-fold quenching (data not shown). The addition of 35% TFE resulted in a 2-nm blue shift in the steady-state emission maximum of NATA. Values for the decay times observed from the hPTH fragments in 35% TFE, corrected by the factor 1.33, are given in parentheses (Table I).

In the presence of the denaturant 6 M GuHCl, hPTH and hPTH 1–34 exhibited quenched fluorescence decay times and changes in their relative contributions in comparison with the results for aqueous solution. This is illustrated in Figure 2 in which the DAS of hPTH in the presence and absence of denaturant are compared. The fluorescence properties of NATA were largely unaffected by 6 M GuHCl. For example, there was no change in the emission maximum (353 nm), and the fluorescence decay indicated a single lifetime of 2.95 ns, a mere 3% quenching (data not shown).

On complexation with acidic lipids, PTH and its deletion analogues displayed largely equivalent fluorescence decay parameters. The shifts in steady-state emission maxima on lipid binding were relatively small, 4–5 nm for hPTH and hPTH 1–34 and 8 nm for hPTH 13–34. Fluorescence titration experiments with POPS established that the complexation was essentially complete at a lipid to peptide ratio of 10:1 (A. G. Szabo and R. Favilla, unpublished observations). The data presented in Table I were obtained at a lipid to peptide ratio of 50:1 to ensure complete complexation. In general, the data for hPTH and hPTH 1–34 in the presence of acidic lipids paralleled the results for aqueous solution.

The fluorescence of rPTH 1–34 was distinct from that of hPTH 1–34. rPTH 1–34 also differed from hPTH 1–34 in its response to the denaturant 6 M GuHCl. The fluorescence decay times of rPTH 1–34 were quenched by 6 M GuHCl although there were no significant changes in the relative contributions of the decay time components. Similar behavior upon denaturation was also observed for hPTH 13–34.

DISCUSSION

Small structural alteration of biomolecules, for example, the oxidation of methionine residues (Zull et al., 1990) or, in

[2] The triple-exponential decay model is the simplest model which is consistent with the data presented. We note that this is not a unique interpretation and more complex models may also fit the data.

Table I: Time-Resolved Fluorescence Decay Parameters[a]

peptide[b]	τ_1[c] (ns)	τ_2 (ns)	τ_3 (ns)	f_1[d]	f_2	f_3	c_1[e]	c_2	c_3	λ^1[f] max (nm)	λ^2 max (nm)	λ^3 max (nm)	λ^{ss}[g] max (nm)	χ^2[h]	SVR[i]
(1) hPTH	5.08	2.10	0.42	0.65	0.32	0.03	0.36	0.44	0.20	349	346	331	346	1.03	1.96
(2) hPTH 1–34	5.14	2.23	0.48	0.63	0.34	0.02	0.37	0.46	0.17	349	346	331	346	1.06	1.93
(3) hPTH 1–34, pH 3.6	4.68	2.24	0.46	0.59	0.39	0.02	0.36	0.49	0.15	350	348	334	348	1.08	1.94
(4) hPTH 1–34, 35% TFE	3.79 (5.04)[j]	1.52 (2.02)	0.17 (0.23)	0.63	0.37	0.00	0.33	0.53	0.14	350	342	327	346	1.08	1.79
(5) hPTH 13–34, 35% TFE	3.80 (5.05)	1.48 (2.00)	0.14 (0.19)	0.65	0.34	0.01	0.36	0.49	0.15	350	342	327	346	1.07	1.82
(6) hPTH, 6 M GuHCl	4.20 (4.32)	1.74 (1.79)	0.27 (0.28)	0.74	0.25	0.01	0.48	0.39	0.13	350	348	332	349	1.03	1.99
(7) hPTH 1–34, 6 M GuHCl	4.32 (4.44)	1.84 (1.89)	0.30 (0.31)	0.71	0.28	0.01	0.47	0.42	0.11	350	348	332	349	1.05	1.91
(8) hPTH 13–34, 6 M GuHCl	4.07 (4.18)	1.69 (1.74)	0.26 (0.27)	0.73	0.25	0.02	0.48	0.38	0.14	350	348	332	350	1.03	1.99
(9) hPTH 13–34	4.84	2.10	0.32	0.72	0.27	0.01	0.47	0.40	0.13	350	345	328	348	1.11	1.83
(10) hPTH, POPS	6.26	1.99	0.44	0.70	0.26	0.03	0.32	0.41	0.27	347	337	327	341	1.05	1.92
(11) hPTH 1–34, POPS	5.81	1.98	0.45	0.68	0.28	0.04	0.32	0.41	0.27	347	337	327	342	1.05	1.93
(12) hPTH 13–34, POPS	6.51	2.15	0.54	0.65	0.30	0.04	0.28	0.43	0.29	346	345	329	340	1.06	1.90
(13) rPTH 1–34	4.47	1.95	0.34	0.67	0.31	0.02	0.42	0.44	0.14	350	345	331	348	1.04	1.96
(14) rPTH 1–34, 6 M GuHCl	3.64 (3.74)	1.73 (1.78)	0.34 (0.35)	0.68	0.30	0.02	0.44	0.40	0.16	350	345	331	350	1.04	1.93

[a] The excitation wavelength was 295 nm. Parameters are given for a global fit to 11 data sets collected as a function of emission wavelength (310–420 nm, the same emission wavelengths were measured for each sample). Stokes Raman scattering at 328 nm from H_2O was used to determine the instrument response function (fwhm 60 ps). Data were collected at 10 ps/channel in 2048 channels. [b] Peptides were typically at a concentration of 10 μM in 1 mM phosphate. The pH was 7.5 unless otherwise indicated. Unilamellar POPS vesicles in 1 mM phosphate, pH 7.5, were added to give a peptide:lipid ratio of 1:50. [c] Fluorescence decay times recovered from global analysis. The standard errors, derived from the diagonal elements of the covariance matrix in the nonlinear least-squares analysis, are typically $\leq$0.01 ns. [d] The fractional fluorescence of the three decay time components at an emission wavelength of 350 nm. Standard errors (see above) are typically $\leq$0.005. [e] The emission wavelength independent fractional concentrations of the three decay time components (see text). Estimated error $\pm$ 0.01. [f] Approximate emission maximum of the spectrum associated with a specified decay time component. [g] Steady-state emission maximum (corrected for instrumental distortion). Estimated error $\pm$ 1 nm. [h] The reduced χ^2 for the global fit (χ^2 = 1 for an ideal fit). [i] The serial variance ratio for the global fit (SVR = 2 for an ideal fit). [j] Values given in parentheses are corrected for the observed quenching of *N*-acetyltryptophanamide in the same solvent system (scale factor 1.33 for 35% TFE and 1.03 for 6 M GuHCl).

the case of synthetic peptides, incomplete deprotection, side reactions, etc., may not easily be detected by conventional methodologies such as HPLC or amino acid analysis. ESI-mass spectrometry was used to confirm the composition of the key samples. This recently developed technique [see Jardine (1990)] allows the determination of the molecular weights of proteins, without fragmentation, to better than 0.01% accuracy. We found that "pure" synthetic peptide samples were frequently contaminated with varying amounts of material having slightly higher or lower molecular weight than that expected. Similar results were reported by Smith et al. (1990) for synthetic hPTH 1–44. The samples used in this study had a mass purity of at least 90%.

The aim of this investigation was to exploit the fluorescence properties of the single tryptophyl residue at position 23 of hPTH to probe local conformational features and the nature of the changes induced by different solvents and by fragmentation of the hormone. A starting point is hPTH in aqueous solution, pH 7.5. The observed steady-state fluorescence emission maximum of 346 nm, in agreement with the data of Brewer et al. (1974), is typical of a solvent-exposed tryptophyl residue. Time-resolved measurements revealed triple-exponential decay kinetics, the relative contributions and associated spectra (DAS) of the decay components are shown in Figure 2. If we compare these parameters with the corresponding values for hPTH 1–34 in the same solvent (Table I), it is apparent that they are closely similar, strongly suggesting that the 35–84 sequence in hPTH has no significant effect on the structure or environment of the 1–34 sequence, at least in the region of residue 23. This result is consistent with earlier reports that the structure (Zull et al., 1990; Neugebauer et al., 1992) and function [see Jüppner (1989)] of hPTH are mainly confined to the 1–34 region. It is also of interest to note that alignment of the 5 known PTH sequences shows that 20 of the 32 conserved residues are found within the 1–34 region of the 84 amino acid polypeptides (K. J. Willis and M. Zuker, unpublished observations).

NMR studies (Smith et al., 1987; Coddington & Barling, 1989) found evidence for pH-dependent structural changes in hPTH 1–34 over the range pH 3–7. The CD difference spectrum (pH 7 – pH 3) for hPTH 1–34 resembles that of an α-helix (Figure 1), and this transition is characterized by a single pK_a of 5.4 $\pm$ 0.1. According to the analysis method of Taylor and Kaiser (1987), the change in mean residue ellipticity (2.1×10^3 deg cm^2 dmol^{-1} at 222 nm) is consistent with the loss of only two helical residues at pH 3. A two-dimensional NMR investigation, of hPTH 1–34 at pH 3 (Lee & Russell, 1989), found no evidence for the α-helical content of 7–11 residues determined from CD data collected at neutral pH (Zull et al., 1990; Cohen et al., 1991; Neugebauer et al., 1991). Our results suggest that the discrepancy between the two techniques can not be fully accounted for by a pH-dependent loss of α-helix (Cohen et al., 1991).

The origin of the single pK_a of 5.4 is unclear, since the value is somewhat high for an acidic residue and low for a histidine. According to the NMR data of Smith et al. (1987), one of the three histidine residues in hPTH 1–34 has a pK_a of 6.8, the other two titrating with a pK_a of 6.3. The glutamate residue at position 22 cannot be responsible since rPTH 1–34, in which Glu-22 is replaced by Gln, shows analogous CD properties and pH behavior.

Fluorescence parameters for hPTH 1–34 at pH 3.6 (Table I) are generally similar to the corresponding values at pH 7.5. Partial protonation of the adjacent Glu-22 probably accounts for the 9% quenching of the long decay time component (Feitelson, 1970). The quenching also resulted in a slightly reduced fractional fluorescence contribution for this decay component; note, however, that the fractional concentrations (see below) are largely unaffected by the pH change. This observation is in accord with the NMR study at pH 3 (Lee & Russell, 1989) which found that a local "non-random" structure in the 20–24 region, first detected at neutral pH (Bundi et al., 1976, 1978), persisted at pH 3. It also suggests that the loss of helical content over the pH range 7–3 occurs in another part of the molecule.

The solvent TFE induces hPTH 1–34 to adopt a more ordered structure. This ordered structure is largely helical according to CD studies (Cohen et al., 1991; Neugebauer et

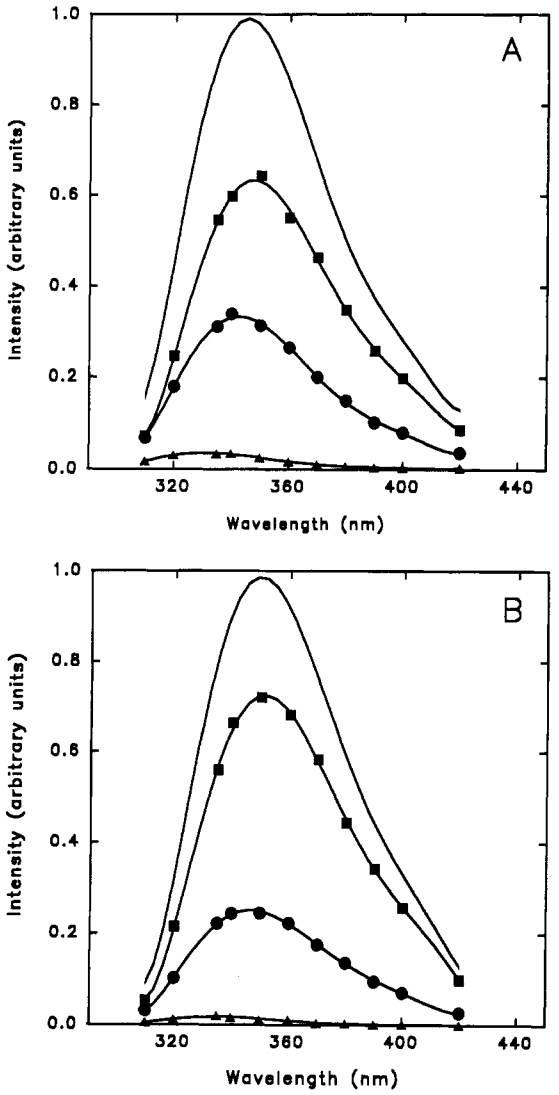

FIGURE 2: Decay-associated emission spectra for hPTH excited at 295 nm. (A) Peptide in 1 mM phosphate, pH 7.5. (B) Peptide in 1 mM phosphate, pH 7.5, containing 6 M GuHCl. Steady-state spectra are indicated by a solid line with no symbols. The squares, circles, and triangles represent in (A) the 5.08-, 2.10-, and 0.42-ns decay time components and in (B) the 4.20-, 1.74-, and 0.27-ns decay time components, respectively. DAS-propagated errors, computed from the standard errors of the fractional fluorescences, are within the contours of the plotted symbols.

al., 1992), and the effect reaches a plateau at a TFE concentration of approximately 35%. An NMR structure for hPTH 1–34 in 11% TFE (Klaus et al., 1991) shows a linear molecule containing two α-helices, residues 3–9 and 17–28, joined by a nonstructured region. It is likely, therefore, that Trp-23 is in an α-helical conformation in 35% TFE.

In addition to its effect on the peptide conformation, TFE also quenches Trp fluorescence. After correction for this general solvent quenching, on the basis of data from a model compound, the fluorescence parameters for hPTH 1–34 in 35% TFE were very similar to those observed in the absence of this solvent. This suggests that the local structure probed by Trp-23 in hPTH 1–34 is unaffected by TFE, implying that this region of the peptide also exists in a largely α-helical conformation in aqueous solution.

Further evidence to support the presence of ordered structure in the region of position 23 in aqueous hPTH 1–34 is provided by the fluorescence data for the peptide in 6 M GuHCl. This denaturant is well suited to fluorescence studies since it has virtually no effect on the fluorescence properties of the model compound NATA. Previous biophysical studies have shown that GuHCl at 6 M concentration disrupts organized structure in PTH (Brewer et al., 1974; Smith et al., 1987). In this study, significant changes in both the decay times and their relative contributions were observed for hPTH 1–34 on addition of 6 M GuHCl.

In Table I, the first nine entries appear to fall into two separate groups. Entries 1–5 have similar fluorescence parameters, and since they include the data for the PTH peptides in 35% TFE, it is proposed that they are characteristic of Trp-23 in an α-helical conformation. Entries 6–9 also have similar fluorescence parameters, but are distinct from those of entries 1–5. Since the former group includes the data for the PTH peptides in 6 M GuHCl, we proposed that in this case the fluorescence parameters reflect an unordered Trp-23 conformation.

It is interesting to note that the fluorescence properties of hPTH 13–34 in aqueous solution were largely unaffected by the presence of 6 M GuHCl. Since hPTH 13–34 behaves analogously to the longer peptides in both 35% TFE and 6 M GuHCl, this result suggests that in aqueous solution the helical-like structure in the region of position 23 is not predominant in the 13–34 fragment. A reduced α-helical content in hPTH 13–34 compared to hPTH 1–34 is also indicated by their respective CD spectra (Figure 1) and has been presented as evidence for α-helical content in the 1–12 sequence (Zull et al., 1990). The fluorescence results demonstrate that it cannot be assumed that fragments will display the same local structural features as the corresponding sequence in the intact molecule.

According to CD data, complexation with POPS vesicles results in a doubling of the α-helical content in hPTH, hPTH 1–34, and hPTH 13–34, indicating a significant interaction (Neugebauer et al., 1992). The lipid-bound fluorescence parameters of the three PTH peptides were found to be very analogous. Contrary to the increase in secondary structure, the fluorescence properties, while not identical, paralleled the values observed in solution with the exception of the 13–34 fragment. The results for the lipid-bound state are therefore consistant with the earlier findings concerning the significance of the 35–84 sequence, the likely helical nature of the probed local structure, and the stability of this local structure in the aqueous 13–34 fragment.

The hPTH 1–34 fragment has a regular distribution of hydrophobic amino acid residues along the entire peptide chain and has the potential to form an amphiphatic helix (Epand et al., 1985). Helical net projections of the 1–34 sequence illustrate that Trp-23 would be in a largely zwitterionic helix and adjacent to a triad of positive charges (residues 25–27). These features suggest that in the lipid-bound state Trp-23 would likely be located near the outer surface of the membrane in the aqueous milieu (Segrest et al., 1990). The fluorescence data (λ_{max} = 341 nm) clearly support this proposal.

In the preceding discussion, we have attempted to establish a correlation between the likely structure of the peptide in the region of the tryptophyl residue and the observed fluorescence properties. The fractional concentrations of the three decay times, c_i, appear to reflect the expected structural differences more consistantly than the changes in the decay times. For example, in Table I the c_1 values for entries 1–5 (Trp-23 main-chain conformation "helical") have a mean of 0.36 with limits of error of ±0.02 at the 0.95 probability level, while the mean for entries 6–9 (Trp-23 "unordered" is 0.48 ± 0.01. It is important, therefore, to comment on the physical significance of this parameter.

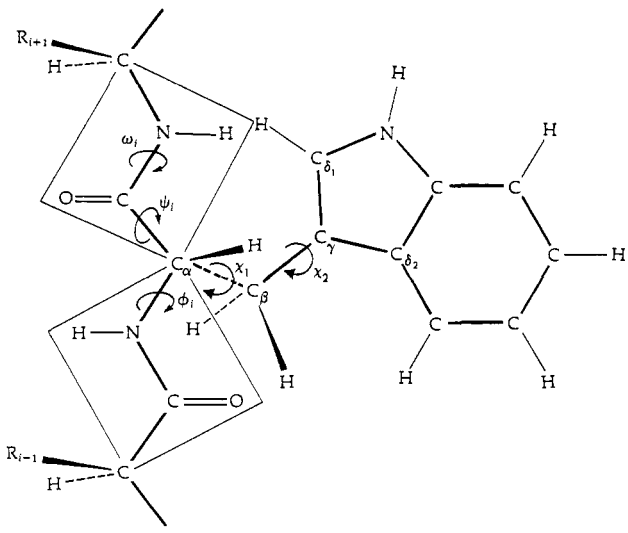

FIGURE 3: Nomenclature for defining the geometry of rotation of a tryptophyl residue. Following the recommendations of the IUPAC–IUB Commission on Biochemical Nomenclature (1970), the C_α–C_β rotamers are defined by the angle $\chi^1 \equiv N$–C_α–C_β–C_γ dihedral angle. The rotamers g^+, g^-, and t correspond to $\chi^1 = 60° \pm 60°$, $-60° \pm 60°$, and $180° \pm 60°$, respectively. C_β–C_γ rotamers are defined by the angle $\chi^2 \equiv C_\alpha$–C_β–C_γ–$C_{\delta 2}$ dihedral angle. The two minimum energy conformations, perpendicular and antiperpendicular, are near $\chi^2 = 90°$ and $-90°$, respectively. In the diagram, the t rotamer is illustrated with χ^2 at an unfavorable 180°.

The derivation of the c_i's assumed that the complex fluorescence decay kinetics were due to ground-state heterogeneity,[3] resulting from the presence of distinct conformers of the Trp-23 side chain, each having different decay times (Donzel et al., 1974; Szabo & Rayner 1980). In this model, the c_i's correspond to the relative conformer, or rotamer, populations. Surveys of crystal structures of proteins (Janin et al., 1978; Bhat et al., 1979; Ponder & Richards, 1987) and oligopeptides (Benedetti et al., 1983) have shown that the side chains of amino acid residues exhibit marked preferences for a small number of configurations corresponding to the fully staggered rotamers. For example, Ponder and Richards (1987) found that the C_α–C_β rotamers of 29 Trp residues were tightly clustered into 3 configurations of relative frequency 0.26 (g^+), 0.47 (g^-), and 0.26 (t). (See Figure 3 for a description of the C_α–C_β rotamers.) The observed conformational distributions can be predicted on the basis of simple steric considerations [see Vásquez et al. (1983) and refrences cited therein].

Recently, direct corrections between the fluorescence decay kinetics and NMR-determined Trp side-chain conformations have been established. Specifically, the normalized preexponential[4] terms were found to have the same value as the NMR-determined relative C_α–C_β rotamer populations [Ross et al., 1992; see also Colucci et al. (1990)]. A 20–24 fragment of hPTH has been studied in detail by NMR (Bundi et al., 1978). Three C_α–C_β rotamers were found for the Trp-23 indole side chain of relative population 0.37 (g^+), 0.47 (g^-), and 0.16 (t). These values are remarkably similar to the fractional concentrations of the three decay times observed for aqueous hPTH 1–34.

Can the rotamer model account for the changes in the fractional concentrations which appear to be correlated with the helix to random-coil transition? Side chains restrict the ϕ, ψ conformational space such that the observed dihedral angles for the peptide bonds fall into the three general regions: right- or left-handed α-helicies and the extended β-structure (Ramachandran et al., 1963). (Dihedral angles in these regions do not necessarily imply secondary structure.) Main-chain peptide bonds attached to the α-carbon, with positions defined by the ϕ, ψ dihedral angles, restrict rotation of the side-chain C_α–C_β bond due to interactions with the atoms at the γ-position (see Figure 3). There is therefore a correlation between main-chain conformation and side-chain rotamer populations (Janin et al., 1978; Benedetti et al., 1983; Vásquez et al., 1983).

For example, the data of Janin et al. (1978) suggest that the transition from a right-handed α-helix to an extended β conformation (averaged over 12 residue types including Trp, 1500 residues total) would decrease the g^- population by 7%, the g^+ population would remain unchanged, and the t population would increase 7%. [The Janin et al. (1978) paper defines g^+ and g^- oppositely to the convention adopted here.] These values may be compared with the ca. 10% average decrease in c_1, 10% increase in c_2, and 3% decrease in c_3 between entries 1–5 (Trp-23 main-chain conformation "helical") and 6–9 (Trp-23 main-chain conformation "unordered") of Table I. While it seems likely that the fractional concentrations are correlated with the C_α–C_β rotamer populations, we are reluctant to attempt to make specific assignments in the absence of direct rotamer population data for the actual systems we have studied by fluorescence spectroscopy. The influence of the C_β–C_γ rotamers on the fluorescence decay kinetics of Trp residues is not clear (Engh et al., 1986; Gordon et al., 1992) although it appears to be secondary to that of the C_α–C_β rotamers (Ross et al., 1992).

From the survey of Janin et al. (1978), the identities of the i+1 and i–1 residues are not expected to directly influence the side-chain rotamer populations adopted by an amino acid residue. In rPTH, the local sequence in the region of Trp-23, R^{20}-M-Q-W-L-R-K^{26}, differs from that of hPTH, R^{20}-V-E-W-L-R-K^{26}, and distinct fluorescence decay parameters were found (Table I). The data for rPTH1–34 more closely resembled those observed for hPTH 1–34 under denaturing conditions. Also, in contrast to hPTH 1–34, the rPTH 1–34 fractional concentrations were largely unchanged following denaturation. This suggests that despite the similarity of their CD spectra the local structure detected by fluorescence in hPTH is not present in rPTH. As the CD spectrum is the average of contributions from all of the residues in the peptide, a localized structural difference may not give rise to significant spectral changes. A helical main-chain conformation in the region of Trp-23 of hPTH could potentially allow a Glu-22 (i) to Lys-26 (i+4) salt bridge, which may be involved in stabilizing the local structure. This salt bridge cannot be present in rPTH owing to the Glu-22 to Gln substitution.

While it is clear that TFE and acidic lipids can stabilize the helical structure in hPTH 1–34, the extent of organized structure in aqueous solution is less certain. Our fluorescence results are consistent with the NMR study of Lee and Russell (1989) which found no detectable secondary structure with the exception of a local nonrandom structure around Trp-23. It has been suggested that this region in PTH and a related sequence in glucagon may be important in receptor recognition and could also serve as a nucleus for conformational rearrangements on binding (Sasaki et al., 1975; Boesch et al., 1978).

[3] Decay measurements at the red edge of the PTH fluorescence emission, in D_2O solution, showed no evidence for excited-state reaction (Willis et al., 1991).

[4] In the study of Ross et al. (1992), the DAS had the same shape and therefore $\alpha_i \equiv c_i$.

A model for the solution structure of hPTH proposed by Zull et al. (1990) assigns a "random" structure to the 19–34 sequence in aqueous solution and suggests that residues 6–12 are helical. This model was based on CD investigations of PTH fragments in which it was assumed that their structures were unchanged from that of the corresponding sequence in the intact molecule. As our data suggest, this may not be the case. Our CD results also suggest that the peptides used in the Zull et al. (1990) study may not have been fully dissolved. Furthermore, the deconvolution of the CD spectra of small peptides, in the absence of a strong α-helical CD pattern, is uncertain (Woody, 1985).

Owing to its location in the molecule, Trp-23 fluorescence gives little information on the structure of the N-terminal sequence of hPTH. Our data provide no evidence for extensive interaction between the N- and C-terminal regions of hPTH 1–34, to form a hydrophobic core, as indicated by the "compact paired helix" model of Cohen et al. (1991).

In conclusion, we have shown that fluorescence studies can complement other spectroscopic techniques such as CD and NMR in the determination of the conformations of peptide hormones. It is often advantageous to be able to probe local structure and interactions at a defined location in the peptide, particularly within a functionally significant domain. This study has provided new information on the structural changes in the region of residue 23 of hPTH induced by sequence deletion, by changes in solvent composition, and by complexation with acidic lipids. Additionally, the results suggest that the fluorescence decay kinetics of a tryptophyl residue can be correlated with the main-chain conformation and therefore potentially report on the local secondary structure. If this proves to be correct, it will be of considerable value in defining the conformation of tryptophyl residues in, for example, peptide agonists and antagonists. It could also be important in protein folding studies. This is illustrated by recent data on the temperature denaturation of staphylococcal nuclease (which has a single Trp). Eftink et al. (1991) reported significant changes in the preexponential terms, but not in the fluorescence decay times, on denaturation.

ACKNOWLEDGMENT

The technical assistance of D. T. Krajcarski is gratefully acknowledged. We thank Drs. A. Ito and R. Favilla for their help in preliminary studies. We also thank Dr. M. Zuker for sequence alignment data, Dr. S. Hasnain for the analysis of pH titration data, and Dr. M. Yaguchi for performing the ESI mass spectroscopy. Dr. J. B. A. Ross and co-workers provided us with a copy of their manuscript prior to publication, for which we are grateful.

REFERENCES

Barden, J. A., & Kemp, B. E. (1989) *Eur. J. Biochem. 184*, 379–394.

Benedetti, E., Morelli, G., Nemethy, G., & Scheraga, H. A. (1983) *Int. J. Pept. Protein Res. 22*, 1–15.

Bhat, T. N., Sasisekharan, V., & Vijayan, M. (1979) *Int. J. Pept. Protein Res. 13*, 170–184.

Boesch, C., Bundi, A., Oppliger, M., & Wüthrich, K. (1978) *Eur. J. Biochem. 91*, 209–214.

Brewer, H. B., Fairwell, T., Rittel, W., Littledike, T., & Arnaud, C. D. (1974) *Am. J. Med. 56*, 759–766.

Bundi, A., Andreatta, R., Rittel, W., & Wüthrich, K. (1976) *FEBS Lett. 64*, 126–129.

Bundi, A., Andreatta, R. H., & Wüthrich, K. (1978) *Eur. J. Biochem. 91*, 201–208.

Caulfield, M. P., McKee, R. L., Goldman, M. E., Duong, L. T., Fisher, J. E., Gay, C. T., DeHaven, P. A., Levy, J. J., Roubini, E., Nutt, R. F., Chorev, M., & Rosenblatt, M. (1990) *Endocrinology 127*, 83–87.

Cavatorta, P., Sartor, G., Neyroz, P., Farruggia, G., Franzoni, L., Szabo, A. G., & Spisni, A. (1991) *Biopolymers 31*, 653–661.

Chakravarthy, B. R., Durkin, J. P., Rixon, R. H., & Whitfield, J. F. (1990) *Biochem. Biophys. Res. Commun. 171*, 1105–1110.

Coddington, J. M., & Barling, P. M. (1989) *Mol. Endocrinol. 3*, 749–753.

Cohen, F. E., Strewler, G. J., Bradley, M. S., Carlquist, M., Nilsson, M., Ericsson, M., Ciardelli, T. L., & Nissenson, R. A. (1991) *J. Biol. Chem. 266*, 1997–2004.

Colucci, W. J., Tilstra, L., Sattler, M. C., Fronczek, F. R., & Barkley, M. D. (1990) *J. Am. Chem. Soc. 112*, 9183–9190.

Donzel, B., Gauduchon, P., & Wahl, Ph. (1974) *J. Am. Chem. Soc. 96*, 801–808.

Eftink, M. R. (1991) *Methods Biochem. Anal. 35*; 127–205.

Eftink, M. R., Gryczynski, I., Wiczk, W., Laczko, G., & Lakowicz, J. R. (1991) *Biochemistry 30*, 8945–8953.

Engh, R. A., Chen, L. X.-Q., & Fleming, G. R. (1986) *Chem. Phys. Lett. 126*, 365–372.

Epand, R. M., Epand, R. F., Hui, S. W., He, N. B., & Rosenblatt, M. (1985) *Int. J. Pept. Protein Res. 25*, 594–600.

Evely, R. S., Bonomo, A., Schneider, H.-G., Moseley, J. M., Gallagher, J., & Martin, T. J. (1991) *J. Bone Miner. Res. 6*, 85–93.

Feitelson, J. (1970) *Isr. J. Chem. 8*, 241–252.

Gordon, H. L., Jarrell, H. C., Szabo, A. G., Willis, K. J., & Somorjai, R. L. (1992) *J. Phys. Chem. 96*, 1915–1921.

Habener, J. F., Rosenblatt, M., & Potts, J. T., Jr. (1984) *Physiol. Rev. 64*, 985–1053.

Hong, B.-S., Yang, M. C. M., Liang, J. N., & Pang, P. K. T. (1986) *Peptides (N.Y.) 7*, 1131–1135.

IUPAC–IUB Commission on Biochemical Nomenclature (1970) *Biochemistry 9*, 3471–3479.

Janin, J., Wodak, S., Levitt, M., & Maigrett, B. (1978) *J. Mol. Biol. 125*, 357–386.

Jardine, I. (1990) *Nature 345*, 747–748.

Jouishomme, H., Whitfield, J. F., Chakravarthy, B., Durkin, J. P., Isaacs, R. J., MacLean, S., Neugebauer, W., Willick, G., & Rixon, R. H. (1991) *Endocrinology 130*, 53–60.

Jüppner, H. (1989) in *Peptide Hormones as Prohormones: Processing, Biological Activity, Pharmacology* (Martinez, J., Ed.) pp 325–354, John Wiley & Sons, Chichester, U.K.

Klaus, W., Dieckmann, T., Wray, V., & Schomburg, D. (1991) *Biochemistry 30*, 6936–6942.

Knutson, J. R., Walbridge, D. G., & Brand, L. (1982) *Biochemistry 21*, 4671–4679.

Knutson, J. R., Beechem, J. M., & Brand, L. (1983) *Chem. Phys. Lett. 102*, 501–507.

Lee, S. C., & Russell, A. F. (1989) *Biopolymers 28*, 1115–1127.

Martin, T. J., Moseley, J. M., & Gillespie, M. T. (1991) *Crit. Rev. Biochem. Mol. Biol. 26*, 377–395.

Nemani, R., Wongsurawat, N., & Armbrecht, H. J. (1991) *Arch. Biochem. Biophys. 285*, 153–157.

Neugebauer, W., Surewicz, W. K., Gordon, H. L., Somorjai, R. L., Sung, W., & Willick, G. E. (1992) *Biochemistry 31*, 2056–2063.

Ponder, J. W., & Richards, F. M. (1987) *J. Mol. Biol. 193*, 775–791.

Potts, J. T., Jr., Kronenberg, H. M., & Rosenblatt, M. (1982) *Adv. Protein Chem. 35*, 323–396.

Ramachandran, G. N., Ramakrishnan, C., & Sasisekharan, V. (1963) *J. Mol. Biol. 7*, 95–99.

Ross, J. B. A., Wyssbrod, H. R., Porter, R. A., Schwartz, G. P., Michaels, C. A., & Laws, W. R. (1992) *Biochemistry 31*, 1585–1594.

Sasaki, K., Dockerill, S., Adamiak, D. A., Tickle, I. J., & Blundell, T. (1975) *Nature 257*, 751–757.

Segrest, J. P., DeLoof, H., Dohlman, J. G., Brouillette, C. G., & Anantharamaiah, G. M. (1990) *Proteins Struct., Funct., Genet. 8*, 103–117.

Smith, L. M., Jentoft, J., & Zull, J. E. (1987) *Arch. Biochem. Biophys. 253*, 81–86.

Smith, R. D., Loo, J. A., Barinaga, C. J., Edmonds, C. G., & Udseth, H. R. (1990) *J. Am. Soc. Mass Spectrom. 1*, 53–65.

Strickler, S. J., & Berg, R. A. (1962) *J. Chem. Phys. 37*, 814–822.

Suva, L. J., Winslow, G. A., Wettenhall, R. E. H., Hammonds, R. G., Moseley, J. M., Diefenbach-Jagger, H., Rodda, C. P., Kemp, B. E., Rodriguez, H., Chen, E. Y., Hudson, P. J., Martin, T. J., & Wood, W. I. (1987) *Science 237*, 893–896.

Szabo, A. G., & Rayner, D. M. (1980) *J. Am. Chem. Soc. 102*, 554–563.

Szabo, A. G., Willis, K. J., Krajcarski, D. T., & Alpert, B. (1989) *Chem. Phys. Lett. 163*, 565–570.

Taylor, J. W., & Kaiser, E. T. (1987) *Methods Enzymol. 154*, 473–498.

Vásquez, M., Nemethy, G., & Scheraga, H. A. (1983) *Macromolecules 16*, 1043–1049.

Willis, K. J., & Szabo, A. G. (1989) *Biochemistry 28*, 4902–4908.

Willis, K. J., Szabo, A. G., & Krajcarski, D. T. (1990) *Photochem. Photobiol. 51*, 375–377.

Willis, K. J., Szabo, A. G., & Krajcarski, D. T. (1991) *Chem. Phys. Lett. 182*, 614–616.

Woody, R. W. (1985) *Peptides (N.Y.) 7*, 15–114.

Zull, J. E., & Lev, N. B. (1980) *Proc. Natl. Acad. Sci. U.S.A. 77*, 3791–3795.

Zull, J. E., Smith, S. K., & Wiltshire, R. (1990) *J. Biol. Chem. 265*, 5671–5676.

Registry No. PTH, 9002-64-6; hPTH 1–34, 52232-67-4; hPTH 13–34, 81306-64-1.